Reliability Engineering and System Safety 229 (2023) 108888

Contents lists available at ScienceDirect

Reliability Engineering and System Safety

journal homepage: www.elsevier.com/locate/ress

# Scenario inference model of urban metro system cascading failure under extreme rainfall conditions

Zhen Yang *, Xiaobin Dong, Li Guo

*College of Resources Engineering, Xi'an University of Architecture and Technology, China*

ARTICLE INFO

*Keywords:*
Extreme rainfall
Metro system
Cascading failure
Interpretive structural modeling
Scenario inference

ABSTRACT

Metro systems have become high-vulnerability entities due to the increasing frequency and severity of urban flooding. Flood events may cause cascading failure to metro systems; therefore, exploring the cascading failure risk of the metro system is a prerequisite for urban flooding prevention and risk management. This study presented a Rank-Order Centroid (ROC) based CIA-ISM (Cross-Impact Analysis, and Interpretive Structural Modeling) method to accurately assess the reliability of emergency management in metro systems under extreme rainfall conditions. We applied this approach to a metro flooding case in Zhengzhou on July 20, 2021. The reliability results show that efficient rescue and timely shutdown notification are the most critical causal events in the cascading failure scenarios. The events of system vulnerability that have the most significant impact on casualties, property losses, and social panic are, respectively, timely notification of the shutdown, humanitarian aid, and public opinion guidance. In forecast scenarios with emergency management measures in effect, the probability of casualties, property losses, and social panic decrease by 96.3%, 58.58%, and 64.28%, respectively. Moreover, a comparison with Bayesian Network (BN) model verified the effectiveness of the ROC-based CIA-ISM approach. Based on the study, we suggest the metro companies release a timely notification of the shutdown. This study can provide scientific data for decision-makers to reasonably develop emergency strategies, significantly reducing flood losses and promoting cities' sustainable development.

## 1. Introduction

Recently, with China's urbanization, many metro lines have been constructed to reduce congestion [1–3]. Metro systems have been the lifelines of megacities, and hazards or incidents involving metro systems will cause severe problems in cities' working and living conditions [4]. The metro systems are considered to be the most significant infrastructures of megacities. However, climate change has profound implications for the effectiveness and viability of critical infrastructures (especially metro systems), making the issue increasingly topical [5]. In 2021 alone, many metropolitan areas in China suffered severe metro flooding. For example, from 16:00 to 17:00, on July 20, the hourly rainfall was 201.9 mm and the passenger flow was 967. Floodwater caused by torrential rain encroached on the tunnel from Shakeoulu and Haitansi stations on Zhengzhou metro line 5. The flood in the metro reached people's necks, causing deaths and five injuries among the more than 500 trapped people [6]. The increasing damage due to extreme rainfall events has forced authorities in flood-prone cities to reevaluate their policy regarding the reliability of metro systems to future heavy rainfall events.

Cascading failure [7] is a kind of failure in a system comprising interconnected parts, in which a part's failure can trigger successive parts' failure. Due to the coupling relationships in complex networks, which are interconnected and continuously generate other nodes. Variations in any one node will affect other nodes potentially in the network; in particular, it will affect unexpected nodes that may amplify the damage of the accident. A well-known phenomenon of cascading is The Butterfly Effect. Cascading failure can be predicted by scenario-based methods, otherwise serious side effects can occur if unpredictable. To address the above issue, numerous scholars have studied the cascading failure of various critical infrastructures using the risk assessment methods, such as Bayesian networks (BNs) [8–10], Directed acyclic graph (DAG) [11–13], Petri Net (PN) [14–16], Markov process (MP) [17–19], etc. Fan et al. [20] proposed a method based on BNs, MP and deep reinforcement learning (DRL) to improve the reliability of supply in natural gas pipeline networks. For a similar problem of pipeline networks [21], the reliability of pipeline networks is optimized by a novel Manifold-based Conditional Bayesian network model. Liu et al.

* Corresponding author.
*E-mail address:* yangzhen@xauat.edu.cn (Z. Yang).

https://doi.org/10.1016/j.ress.2022.108888
Received 18 May 2022; Received in revised form 10 September 2022; Accepted 6 October 2022
Available online 12 October 2022

[22] explored the integration of triangular membership and regional center method to SPN for the modeling and evaluation of gas leakage emergency rescue process in gas transmission station. As the traditional critical infrastructure, the hospital is a crucial social component, especially during the spread of the Coronavirus (COVID-19) pandemic. Liu et al. [23] evaluated the seismic resilience of hospital buildings using BNs, considering the cascading relationships on nonstructural components. Silva et al. [24] proposed reliability and availability models adopting stochastic Petri net (SPN) to quantify the impact of energy resources and rejuvenate medical sensor networks' dependability. Similarly, the cascading failure mode of metro systems has been studied widely. Ye et al. [25] proposed a novel grey- Markov prediction model to describe different contribution degrees of historical information of future change trends of system characteristics. Li and Wu [26] proposed a deep reinforcement learning (RL)-based decision support system for stakeholders to optimally manage the critical components of transportation networks to minimize the network-level losses induced by hurricanes. Ghoushchi et al. [27] proposed a novel approach to select the optimal landfill for medical waste using Multi-Criteria Decision--Making (MCDM) methods. Wang et al. [28] applied the CIA-ISM approach to analyze emergency scenarios. Chen et al. [29] discussed the complex interrelationships among the barriers to building-integrated photovoltaics in Singapore. With the rapid development of technology, the emerging infrastructures, such as the Internet of Things (IoT) [30], cloud data centers [31], electric-cyber infrastructure [32], and computerization in supply chains [33], have aroused wild attention.

In this paper, the metro system is identified as a dynamic one impacted by extreme climate. The analysis of cascading process and the decoupling are complex in this case. Scenario-based methods can clearly describe the cascading failure and coupling mode, which can improve the decoupling efficiency and accuracy. In addition, system elements are difficult to quantify. Therefore, they are simplified into events. The system components involved in the cascading process are in the form of events, which reduce the computational dimension.

This study aims to address the research gaps inherent in the previous researches, which are summarized as follows:

1. Cascading failure analysis in the metro system has been conducted based on research with interaction coupling relationships and decoupling among system elements. With the development of extreme climate, the analysis of cascading failure mode becomes difficult in complex systems. Hence, how to properly assess the cross-impact relationships between essential events places an emerging challenge for the research into cascading failure.

2. Emergency measures are critical factors in reducing losses under extreme rainfall conditions. However, when investigating metro flooding risk, few studies have attempted to assess the efficiency of emergency management measures. Therefore, how to precisely analyze the priority and efficiency of emergency measures is the problem to be resolved in this study, which we believe is essential to the cascading failure research on metro systems.

3. In most studies, the CIA-ISM method's event probabilities are determined in two ways: assessed by historical case data and the Delphi method. The former CIA-ISM has accurate results but it is always hard to collect data, while the latter method is efficient in assessment but usually has violent subjectivity. Therefore, it is necessary to develop a scenario-based method that makes a trade-off between veracity and objectivity.

In this study, we focus on the metro systems under extreme rainfall conditions as the unit of analysis and regard excessive rainfall as the external perturbation of the system. Then based on the conventional CIA-ISM model, the ROC-based CIA-ISM model is proposed to infer the cascading failure scenario process in metro systems under extreme rainfall conditions, especially the cross-impact relationships between critical events. Finally, several representative scenario graphs are built to predict the influence of the specific events on the outcome events[1]. Furthermore, we adopt the BN model to demonstrate the efficiency of the ROC-based CIA-ISM. The findings can provide suggestions for metro management and emergency repair strategies for the metro system department under extreme rainfall conditions.

Our main contributions to this paper are:

We adopt the ROC method that was originally developed in multi-criteria decision analysis (MCDA) for the elicitation of criteria weight, which turns ordinal judgments into ratio-scale information [34–36]. This type of elicitation only requires experts to provide a ranking of events according to their likelihood, providing a fast and nonnumerical elicitation process. Probabilities are subsequently approximated from the ranking by an algorithm based on the principle of maximum entropy. By using the ROC-based CIA-ISM method, we could fast obtain the initial probability of events. In addition, we could accurately assess the scenario inference process of cascading failure in complex systems and improve their evaluation efficiency.
The adoption of the ROC-based CIA-ISM approach that we proposed in this article was able to assess the reliability of critical emergency measures in metro systems under extreme rainfall conditions. We had predictably formalized its use for the ranking of emergency measures. In addition, we extended the prediction scale, so it could also estimate the efficiency of emergency management measures in complex systems comprehensively. Furthermore, we provided several special emergency measures, indicating their significance.
Using a simulation study, we tested the priority of emergency events under three outcome conditions. We compared the method to BN model and find that the proposed method is more accurate than the scenario-based method that we test. We took the ROC-based CIA-ISM approach in practice and adopted it to the "7.20" accident to get the cascading failure process, and gave some advices.

The rest of the paper is organized as follows: Section 2 describes the methodology we developed to perform the cascading failure analysis; Section 3 describes the test case used to demonstrate the applicability of the developed method; The analysis and results are presented in Section 4; Section 5 presents the conclusions.

## 2. Methodology

The ROC-based CIA-ISM model introduced in this paper comprises the Rank-order centroid method and the CIA-ISM model. Fig. 1 shows the collaborative modeling process based on the ROC-based CIA-ISM model.

### 2.1. Rank-order centroid method

ROC is a method to obtain probability derivation based on numerical ordering. The ROC method can get criteria weights, which turns ordinal judgments into ratio-scale information [34–37]. This type of elicitation only requires experts to rank events according to their likelihood, providing a fast and nonnumerical elicitation process. Probabilities are subsequently approximated from the ranking by an algorithm based on the principle of maximum entropy [38].

ROC can be used to elicit the probabilities for four different types of events: mutually exclusive binary events, the probability density function of one variable, stochastically independent binary events, and low-probability binary events.

(1) Mutually exclusive binary events

[1] The outcome events represent the categories of events.

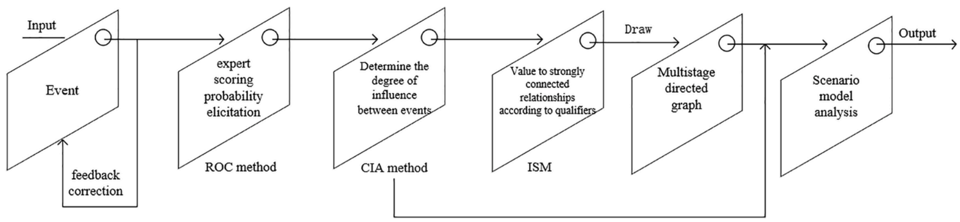


**Fig. 1.** Collaborative modeling flow chart of the ROC-based CIA-ISM model.

Experts are given the list of binary events *S1, S2..., Sn* and are asked to rank them according to their likelihood of occurrence; thus, the resulting ranking is consecutively transformed into probabilities. The information given by the experts about the probabilities can be summarized by $P_1 \geq P_2 \geq \ldots \geq P_n$ and $\Sigma P_i = 1$. The average vector obtained by the ROC method contains the probability of each event. An equivalent calculation of each probability individually is given by Eq. (1).

$$P_i = \frac{\sum_{k=i}^{n} \frac{1}{k}}{n} \tag{1}$$

(2) The probability density function of one variable

For events with the probability density function of one variable, the algorithm is the same as the mutually exclusive binary events, and there is no procedural difference.

(3) Stochastically independent binary events

If the events given by experts are stochastically independent binary events, the ranking of events is transformed into probability by the ROC method. The ranking essentially assigns each event in the sample an order statistic, and an order statistic is defined over a statistical sample such that the kth order statistic of a sample is the kth smallest value from that sample [39]. When n values within the unit interval are independently identically distributed, the $i$ ($i \leq n$) th ordered element is the ($n+1-i$) th order statistic of the uniform distribution, which has the expected value of $(n+1-i)/(n+1)$. We can thus assign probabilities for the events by Eq. (2):

$$P_i = \frac{n+1-i}{n+1} \tag{2}$$

(4) Low-probability binary events

The probability of low probability binary events is derived by modifying the methods of 1 and 3. The expert needs to make a numerical assessment of the event and derive $P_0$ using conventional probabilistic methods—the probability that none of the specified events occurs. When events are mutually exclusive, the$\Phi$-measures (so called$\Phi$-measures, which are similar to the relative likelihood measures used by Ludke et al. [40]) have the same relative magnitudes toward each other as the probabilities given by Eq. (1). $\Phi_i$ is calculated by Eq. (3):

$$\phi_i = \frac{\sum_{k=i}^{n} \frac{1}{k}}{\sum_{j=1}^{n} \frac{1}{j}} \tag{3}$$

Eq. (4) should be employed in the case of stochastically independent events.

$$\phi_i = \frac{n+1-i}{n} \tag{4}$$

The measures calculated by these equations are not yet probabilities, but the probability $p$ is also a ratio-scale measure of an event's likelihood. The two can be mapped into each other by a positive multiplicative transformation. If a likelihood ratio between events $i$ and $j$ is denoted $b_{ij}$, then:

$$b_{ij} = \frac{P_i}{P_j} = \frac{\phi_i}{\phi_j}$$

Such that in case $j = 1$:

$$b_{i1} = \frac{\phi_i}{\phi_1} = \frac{\phi_i}{1} = \phi_i$$

It follows that Eq. (5):

$$P_i = \phi_i P_1 \tag{5}$$

The$\Phi$-measures can be normalized to derive the respective probabilities. In the case of mutually exclusive events, we take advantage of the fact that the sum of all event probabilities must be equal to $1-P_0$; see Eq. (6):

$$P_i = (1 - P_0) \frac{\phi_i}{\sum_{i=1}^{n} \phi_i} \tag{6}$$

Eq. (7) should be employed in the case of stochastically independent events.

$$\prod_{i=1}^{n} (1 - \phi_i P_1) - P_0 = 0 \tag{7}$$

Because Eq. (7) is an $n$-order polynomial in $P_1$, it can have up to n solutions. In general, $n$-order polynomials do not have an analytical solution for $n$ greater than 4. However, a bisection method for the interval [0,1] can be used to obtain a solution for Eq. (7). Once a $P_1$ is found from solving Eq. (7), the other probabilities follow from Eq. (5).

### 2.2. CIA-ISM model

CIA is a methodology used to help determine how relationships between events affect outcome events, reduce future uncertainty, and predict events based on the nonindependence of events occurring [41]. Experts evaluate the impact relationship between two events according to Table 1 (see Fig. 2 for the evaluation process) and then obtain the estimation matrix as the input of the cross-impact matrix. The cross-impact matrix is established according to the cross-impact formula of Eqs. (8) and (9). The cell in the matrix is the influence factor $C_{ij}$ (representing the influence coefficient on $E_i$), the diagonal cell is the overall probability (*OPV*) , and $G_i$ represents the impact of external events on $E_i$. A positive value of $C_{ij}$ means that the occurrence of $E_j$ can push the occurrence of $E_i$, and a negative value obstructs the occurrence ("positive" and "negative" in this paper indicate the mathematical direction of influence "+" and "−").

$$C_{ij} = \frac{1}{1-P_j}\left[\left(\ln \frac{R_{ij}}{1-R_{ij}}\right) - \left(\ln \frac{P_i}{1-P_i}\right)\right] \tag{8}$$

$i\,j$ represents an event;

$R_{ij}$ represents the impact that the occurrence of $E_j$ may have on the

**Table 1**
Score table.

| Score | Influence degree |
|---|---|
| 0.99 | Significant positive impact[6] |
| 0.9 | Obvious positive impact |
| 0.8 | Great positive impact |
| 0.7 | A certain positive impact |
| 0.6 | Slight positive impact |
| 0.5 | No impact |
| 0.4 | Slight negative impact |
| 0.3 | A certain negative impact |
| 0.2 | Great negative impact |
| 0.1 | Obvious negative impact |
| 0.01 | Significant negative impact[7] |

[6] Positive impact indicate the mathematical direction of influence "+".
[7] Negative impact indicate the mathematical direction of influence "−".

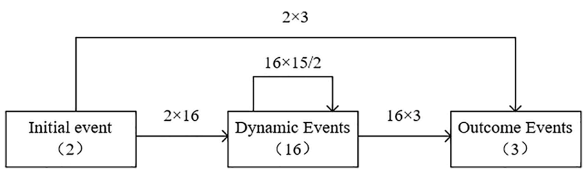


**Fig. 2.** Influence diagram with the number of events and the number of estimates needed.

event of $E_i$;

$P_{i,j}$ represents the probability for the occurrence of $E_{i,j}$.

$$P_i = \frac{1}{1 + \exp\left(-G_i - \sum_{k \neq i} C_{ik} P_k\right)} \tag{9}$$

$P_{i,k}$: represents the prediction probability of $E_{i,k}$;

$G_i$ represents the impact of external events on $E_i$.

ISM is an effective method to analyze and reveal the structure of complex relationships by describing systems and system elements in a matrix and graph based on practical experience. The purpose of the ISM method is to divide the analyzed system into various subsystems, analyze the binary relationship between each factor, reveal the system structure through Boolean logic operation, and present it in the most straightforward hierarchical directed topology diagram.

ISM can graphically express a decision model based on the ROC-based CIA-ISM and construct scenarios through a series of events; see Eq. (10):

$$S = \{S_1, S_2, \ldots, S_n\} \tag{10}$$

There is a binary relation between the elements in the set S. According to the binary link, the adjacency matrix A can be calculated and defined as a binary $n \times n$ matrix. The cell in the matrix is $a_{ij}$, which is calculated by Eq. (11):

$$a_{ij} = \begin{cases} 1, S_i K S_j \\ 0, S_i \overline{K} S_j \end{cases} \tag{11}$$

1 represents the direct connection from node $S_i$ to node $S_j$;

0 represents no direct connection from node $S_i$ to node $S_j$.

Matrix A is calculated by Eq. (12) to obtain reachability matrix R:

$$R = (A + I)^{m+1} = (A + I)^m \neq (A + I)^{m-1} \tag{12}$$

I represent the identity matrix.

The output of CIA is taken as the input of ISM, and the multilevel directed graph is obtained by dividing the hierarchy of the reachable matrix R.

## 3. Test case

Metro stations have strong closure, large passenger flow, complex passenger flow, and difficult emergency evacuation. Once an accident occurs, it quickly causes heavy casualties, induces secondary disasters or derivative disasters, and causes negative social impacts [42]. This paper intends to analyze the scenario evolution and system vulnerability nodes of metro flooding disasters given the cascading failure of metro systems in extreme rainfall. It takes the "7.20" metro flooding accident in Zhengzhou as an example for verification.

### 3.1. Create the accident event set

Events can be divided into three categories according to their nature [43]; see Table 2.

Initial events (IEi): An initial event is a hypothetical prior or source event that has occurred before the disaster or accident and may be true or false before the disaster occurs. Initial events can reflect disaster preparedness and have a potentially significant impact on dynamic events;

Dynamic events (DEi): Dynamic events can be true or false and are related events after the occurrence of disasters;

Outcome Events (OEi): The result of a disaster or accident.

### 3.2. Scenario analysis

After the event set is determined, the initial probability of the possible occurrence of each event is obtained by the ROC method. For lack of data in this field, this paper integrates expert opinions to rank the event sets from high to low. Using Eqs. (4), (5), and (7), the ordering of each event is summarized, and a scientific and rational initial probability table (Table 3) is obtained.

Using Eq. (4) to calculate the φ-ratio, the expert assessed the probability of no uncertain events occurring during the observation period (i.e., $P_0$) as 10% and adjusted the multiplication to 0.143 according to Eq. (7). Finally, the probability of each index is calculated by Eq. (5).

The initial probability and estimation matrix of events obtained by ROC were taken as the input to CIA, and the cross-impact matrix (Table 4) was obtained according to Eq. (8). The value in the cross-

**Table 2**
Set of metro flooding accidents on July 20 in Zhengzhou.

| Event Category | Events | Explanation |
|---|---|---|
| Initial events | IE1 | The maximum daily precipitation of more than 150 mm. |
| | IE2 | Metro flooding occurs during rush hours. |
| Dynamic events | DE1 | The traffic system is paralyzed. |
| | DE2 | Destruction of buildings, such as a rupture, fall, and collapse. |
| | DE3 | Failure of component or structure. |
| | DE4 | Persistent rain. |
| | DE5 | Poor communication or interruption. |
| | DE6 | Heavy rains cause widespread flooding in the area. |
| | DE7 | Professional emergency rescue teams undertake efficient rescue tasks. |
| | DE8 | Humanitarian aid can be delivered to the population. |
| | DE9 | Emergency medical care is provided for victims. |
| | DE10 | The government can guide public opinion and defuse public discontent effectively. |
| | DE11 | The victims have a strong ability to help themselves. |
| | DE12 | The electricity supplies are disrupted. |
| | DE13 | Surface and underground drainage systems are broken. |
| | DE14 | Metro ventilation system failure. |
| | DE15 | The metro company releases a timely notification of the shutdown. |
| | DE16 | Metros are equipped with first aid equipment. |
| Outcome Events | OE1 | Metro flooding causes heavy casualties. |
| | OE2 | Metro flooding causes substantial economic losses. |
| | OE3 | Poor emergency rescue work has caused social panic. |

**Table 3**
Table of case study results.

| Events | Rank | φ-ratio | Pi | Events | Rank | φ-ratio | Pi | Events | Rank | φ-ratio | Pi |
|---|---|---|---|---|---|---|---|---|---|---|---|
| IE1 | Certain | n.a, | 100% | DE6 | 4th | 0.85 | 12.16% | DE13 | 5th | 0.8 | 11.44% |
| IE2 | 6th | 0.75 | 10.73% | DE7 | Certain | n.a, | 100% | DE14 | 12th | 0.45 | 6.44% |
| DE1 | 3rd | 0.9 | 12.87% | DE8 | Certain | n.a, | 100% | DE15 | 2nd | 0.95 | 13.59% |
| DE2 | 8th | 0.65 | 9.30% | DE9 | Certain | n.a, | 100% | DE16 | 17th | 0.2 | 2.86% |
| DE3 | 9th | 0.6 | 8.58% | DE10 | 16th | 0.25 | 3.58% | OE1 | 7th | 0.7 | 10.01% |
| DE4 | 14th | 0.35 | 5.01% | DE11 | 13th | 0.4 | 5.72% | OE2 | 1st | 1 | 14.30% |
| DE5 | 11th | 0.35 | 5.01% | DE12 | 10th | 0.55 | 7.87% | OE3 | 15th | 0.3 | 4.29% |

impact matrix represents the influence degree between events.

To assess the reasonableness of the event set, check the sum of the following factors from Table 4:

| Internal event impacts $|=\Sigma|C_{ij}|=844.85$
| External events impacts $|=\Sigma|G_i|=70.73$
| Total impacts $|=\Sigma|C_{ij}|+\Sigma|G_i|=915.58$
| Internal event impacts |/| Total impacts |=92.27%
| External event impacts |/| Total impacts |=7.73%

The calculations show that events in the event set determine 92.27% of the total impact, and 7.73% is determined by events not included in the event set. This shows that the event set is comprehensive to a certain extent and that the model is feasible. We can obtain the cross-impact matrix set limit $|C_{ij}|$ to focus on the most critical events as the input of ISM (such as in Fig. 3, when extracting the top 30% of the most significant effect, the limit for $|C_{ij}|= 3.41$).

This process aims to obtain a strongly connected structure that describes the relationships between events in a directed graph model. If the $|C_{ij}|$ value is greater than or equal to the limit, $S_j$ said node to node $S_i$ has a direct connection.

The ISM method can represent the forecast scenario with a multilevel directed graph structurally and intuitively displaying the direction and degree of influence between events. Figs. 4 and 5 show the limits $|Cij|=4.17$ (10%) and $|Cij|=3.41$ (30%), respectively, of the directed graph. In the figures, different colors represent different directions of influence. The relationship between two events of the same color indicates a positive influence, while events of different colors denotes a negative influence.

Figs. 4 and 5 reveal cascading failure scenarios in metro systems under extreme rainfall conditions. Fig. 4 shows no DE14 because it weakens relationships with other events ($|Cij| < 4.17$). DE1 and DE4 have the highest coupling degree in cascading failure mode in Fig. 4, indicating that traffic system paralysis and continuous rainfall have the most significant influence on the outcome events. DE2, DE3, DE12, and DE13 followed, indicating that the failure of metro buildings, components, power, and drainage systems caused by heavy rain also significantly impacted the outcome events. IE2 has a direct positive effect on OE1 and OE3, which indicates that metro flooding during rush hours will almost certainly cause casualties and social panic. DE7, DE8, DE9, DE10, DE11, and DE16 have a direct negative impact on the outcome events, indicating that the spread of the outcome events can be effectively contained by efficient rescue tasks and adequate reserve of emergency supplies, and timely assistance from society and government. DE15 has a direct negative impact on casualties and economic losses, which means that the metro company should release a timely notification of the shutdown based on the situation of metro flooding and the precipitation. IE1, DE1, DE2, DE3, DE4, DE5, DE6, DE12, and DE13 indirectly impact the outcome events based on cascading failure mode through DE7.

In Fig. 5, the top 30% of solid relationships are selected to construct the hierarchy, which contains more causal relationships than in Fig. 4, and DE14 is also included. The initial event IE1 has a direct effect on DE12. DE8 and DE9 form a micro scenario, meaning that these two events have a positive impact and usually occur together. The coupling relationship of DE10 increases, indicating that the government's timely guidance of public opinion significantly impacts metro flooding accidents. In all emergency response events, the efficient rescue task undertaken by rescue teams has a direct and vital impact on reducing human casualties (OE1) and alleviating social panic (OE3).

The combination of the ISM output with the results of the CIA is the basis of scenario analysis. This paper aims to evaluate the system vulnerability nodes and reliability of emergency management measures related to metro flooding accidents through cascading failure mode, so relevant events are selected for sensitivity analysis. The initial probability of related events is changed to determine its influence on each event, mainly the result event. Related events are extracted from initial and dynamic events based on event nature. The system vulnerability events related to metro flooding accidents are as follows: IE2, DE1, DE5, DE7, DE8, DE9, DE10, DE15, and DE16. Tables 5 and 6 show the predicted probabilities of initial and dynamic events, respectively.

In initial events, IE2 is related to emergency management. The influence of the critical factor can be tested by changing the initial probability to analyze the consequences for the other events, especially for the outcome events. There are two scenario forecasts in which event IE2 is supposed to apply to the case (1: occurs; 0: does not occur). The initial probability of the other event remains 0.5. Based on the cross-impact formula Eq. (9), the probability of the other events under those two scenario forecasts can be observed in Table 5.

From these results, metro flooding during rush hours (IE2) impacted the outcome events, and from high to low they are OE1, OE2, and OE3. The metro flooding occurrence during non-rush hours is important for reducing casualties (OE1), significantly mitigating economic losses and alleviating social panic. After the meteorological department issues a heavy rainfall warning or before the occurrence of metro flooding, the government and relevant departments should make timely preparations to evacuate people and issue a notice of metro shutdown. The loss can be reduced considerably if the initial event of IE2 does not occur, so timely emergency evacuation by government departments is necessary to enhance the metro system's reliability under extreme rainfall conditions. The vulnerability nodes on the path of cascading failure belonging to IE2 are DE1, DE7, DE8, and DE9 from Fig. 5 and Table 5. IE2 does not cause the change of prediction probability of DE7, DE8, and DE9 because the rescues will not be interrupted when metro flooding occurs. Undoubtedly, the transport system is paralyzed under extreme rainfall conditions, thus hindering the efficiency of the rescues.

Dynamic events related to system vulnerability include DE1, DE5, DE7, DE8, DE9, DE10, DE15, and DE16. The same method can be used to calculate the influence of these key factors on other events, especially the result events. The results are shown in Table 6. S0 indicates that the dynamic events related to system vulnerability are in the state of having a positive impact on the result events OE1, OE2, and OE3; S9 indicates that the dynamic events related to system vulnerability are in the state of hurting the result events OE1, OE2, and OE3; and S1-S8 suggest the condition of each dynamic event related to system vulnerability.

According to S1 in Table 6, compared with other dynamic events, traffic system paralysis caused by heavy rain has a significant impact on human casualties (OE1), economic loss (OE2), and social panic (OE3). Compared with S9, ensuring a smooth traffic system flow in post-disaster rescue has become crucial to reduce casualties and economic losses and alleviate social panic. S2 shows that communication system failure or interruption has also become a key factor leading to deaths

**Table 4**
Cross-impact matrix.

| Events | IE1 | IE2 | DE1 | DE2 | DE3 | DE4 | DE5 | DE6 | DE7 | DE8 | DE9 | DE10 | DE11 | DE12 | DE13 | DE14 | DE15 | DE16 | OE1 | OE2 | OE3 |
|---|---|---|---|---|---|---|---|---|---|---|---|---|---|---|---|---|---|---|---|---|---|
| IE1 | OPV | 0 | 0 | 0 | 0 | 0 | 0 | 0 | 0 | 0 | 0 | 0 | 0 | 0 | 0 | 0 | 0 | 0 | 0 | 0 | 0 |
| IE2 | 0 | OPV | 2.44 | 2.33 | 2.31 | 2.23 | 2.29 | 2.42 | 0 | 0 | 0 | 2.18 | 2.25 | 2.31 | 2.39 | 2.27 | 2.46 | 2.46 | 3.63 | 2.39 | 2.56 |
| DE1 | 0 | 2.14 | OPV | 2.55 | 2.53 | 3.46 | 2.07 | 3.76 | 0 | 0 | 0 | 1.97 | 2.03 | 4.48 | 7.35 | 2.05 | 2.22 | 2.22 | 2.76 | 3.00 | 2.91 |
| DE2 | 0 | 2.55 | 2.62 | OPV | 3.99 | 3.28 | 2.46 | 4.18 | 0 | 0 | 0 | 2.35 | 2.41 | 2.48 | 3.53 | 2.44 | 2.64 | 2.64 | 2.25 | 4.12 | 1.99 |
| DE3 | 0 | 2.65 | 2.72 | 4.13 | OPV | 3.37 | 2.56 | 3.66 | 0 | 0 | 0 | 2.44 | 2.51 | 2.58 | 3.63 | 2.53 | 2.74 | 2.74 | 2.31 | 2.88 | 2.06 |
| DE4 | 0 | 3.30 | 3.38 | 3.24 | 3.21 | OPV | 3.18 | 3.36 | 0 | 0 | 0 | 3.03 | 3.12 | 3.21 | 3.33 | 3.15 | 3.41 | 3.41 | 3.10 | 5.48 | 3.67 |
| DE5 | 0 | 2.42 | 2.95 | 2.82 | 4.31 | 2.69 | OPV | 3.39 | 0 | 0 | 0 | 2.64 | 2.72 | 4.31 | 3.85 | 2.74 | 2.97 | 2.97 | 2.51 | 2.67 | 2.20 |
| DE6 | 0 | 2.22 | 2.27 | 3.11 | 2.60 | 4.38 | 2.14 | OPV | 0 | 0 | 0 | 2.04 | 2.10 | 2.16 | 4.72 | 2.12 | 2.29 | 2.29 | 2.86 | 3.13 | 2.78 |
| DE7 | 0 | 0 | 0 | 0 | 0 | 0 | 0 | 0 | OPV | 0 | 0 | 0 | 0 | 0 | 0 | 0 | 0 | 0 | 0 | 0 | 0 |
| DE8 | 0 | 0 | 0 | 0 | 0 | 0 | 0 | 0 | 0 | OPV | 0 | 0 | 0 | 0 | 0 | 0 | 0 | 0 | 0 | 0 | 0 |
| DE9 | 0 | 0 | 0 | 0 | 0 | 0 | 0 | 0 | 0 | 0 | OPV | 0 | 0 | 0 | 0 | 0 | 0 | 0 | 0 | 0 | 0 |
| DE10 | 0 | 3.69 | 3.79 | 3.62 | 3.59 | 3.46 | 2.06 | 3.76 | 0 | 0 | 0 | OPV | 3.49 | 3.59 | 3.72 | 3.53 | 2.21 | 3.82 | 2.14 | 2.16 | 8.21 |
| DE11 | 0 | 3.59 | 2.76 | 3.08 | 3.05 | 2.94 | 3.03 | 3.19 | 0 | 0 | 0 | 2.89 | OPV | 3.05 | 3.17 | 3.00 | -2.08 | 4.23 | 2.67 | 2.31 | 2.46 |
| DE12 | 0 | 2.76 | 2.83 | 4.23 | 4.19 | 3.01 | 2.66 | 3.77 | 0 | 0 | 0 | 2.53 | 2.61 | OPV | 4.35 | 2.63 | 2.85 | 2.85 | 2.37 | 2.48 | 2.13 |
| DE13 | 0 | 2.29 | 2.35 | 3.78 | 4.63 | 2.57 | 2.21 | 3.91 | 0 | 0 | 0 | 2.11 | 2.17 | 2.23 | OPV | 2.19 | 2.37 | 2.37 | 2.97 | 3.28 | 2.67 |
| DE14 | 0 | 3.00 | 3.08 | 3.88 | 5.31 | 3.24 | 2.89 | 3.51 | 0 | 0 | 0 | 2.76 | 2.84 | 2.92 | 3.48 | OPV | 3.11 | 3.11 | 2.59 | 2.77 | 2.37 |
| DE15 | 0 | 0.52 | 1.15 | 2.97 | 2.46 | 1.94 | 1.08 | 3.08 | 0 | 0 | 0 | 1.91 | 1.96 | 2.02 | 2.09 | 1.98 | OPV | 2.15 | 4.85 | 3.44 | 3.06 |
| DE16 | 0 | 3.95 | 4.05 | 3.88 | 3.84 | 3.70 | 3.81 | 4.02 | 0 | 0 | 0 | 3.63 | 3.74 | 3.84 | 3.98 | 3.77 | 4.09 | OPV | 2.19 | 2.24 | 1.92 |
| OE1 | 0 | 4.92 | 4.12 | 3.35 | 3.32 | 2.73 | 3.29 | 4.08 | 0 | 0 | 0 | 2.26 | 0.00 | 3.32 | 4.05 | 3.26 | -2.78 | 0.94 | OPV | 2.57 | 2.71 |
| OE2 | 0 | 3.56 | 2.53 | 4.39 | 3.46 | 2.77 | 2.85 | 4.55 | 0 | 0 | 0 | 1.84 | 1.00 | 3.46 | 4.51 | 2.82 | 0.47 | 1.09 | 3.71 | OPV | 2.74 |
| OE3 | 0 | 5.94 | 5.17 | 3.86 | 3.83 | 4.72 | 4.85 | 5.12 | 0 | 0 | 0 | -1.53 | 1.82 | 3.83 | 4.47 | 3.76 | 1.05 | 1.99 | 8.05 | 6.20 | OPV |

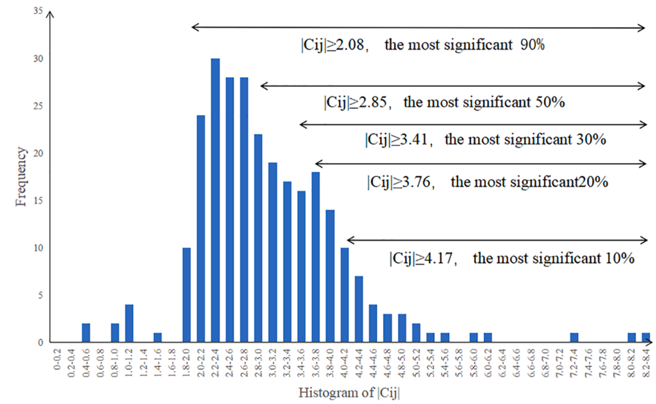


**Fig. 3.** Histogram of the cross-impact factor distribution.

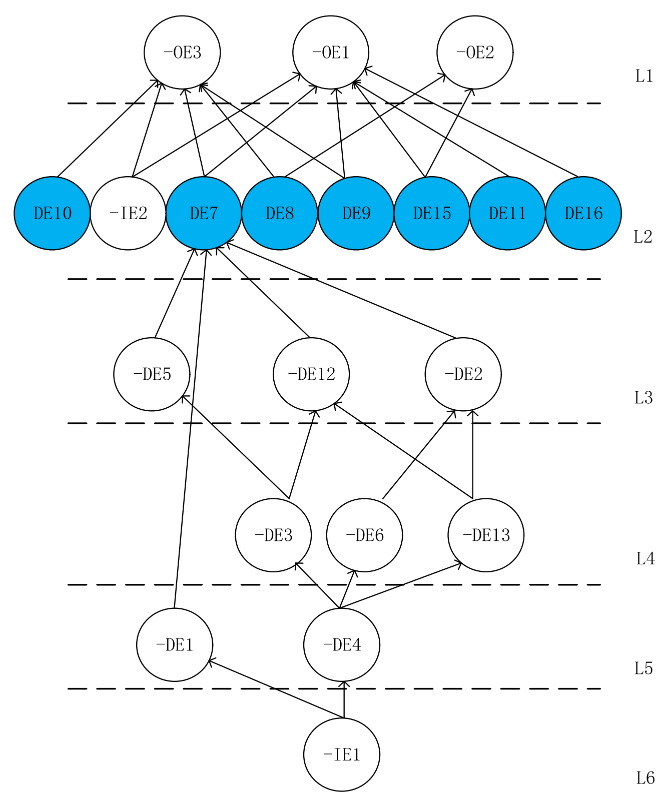


**Fig. 4.** Digraph for the limit value $|C_{ij}| = 4.17$– with 10%.

(OE1), economic losses (OE2), and social panic (OE3) after heavy rain. Compared with S9, it can be seen that the government and relevant departments should rush to repair the communication system in time after the disaster to ensure contact with the people affected. In S3, S4, S5, and S8, the probability of dynamic events DE7, DE8, DE9, and DE16 are equal to 1. This represents an efficient rescue mission, timely humanitarian aid and emergency medical treatment delivery, and complete first-aid tools in metro cars. In this case, human casualties (OE1) and economic losses (OE2) can be greatly reduced, and social panic can be slightly alleviated. S6 represents the DE10=1 scenario. In the case of a single dynamic event, the occurrence of DE10 has the most significant impact on helping social panic. Compared with other events, the timely release of accurate information by the government, guidance of public opinion, and resolution of general dissatisfaction have a more noticeable effect on alleviating social panic. In the scenario S7, the metro administration promptly issued a suspension notice (DE15) in each dynamic event scenario, thus significantly reducing casualties. In S9, all the

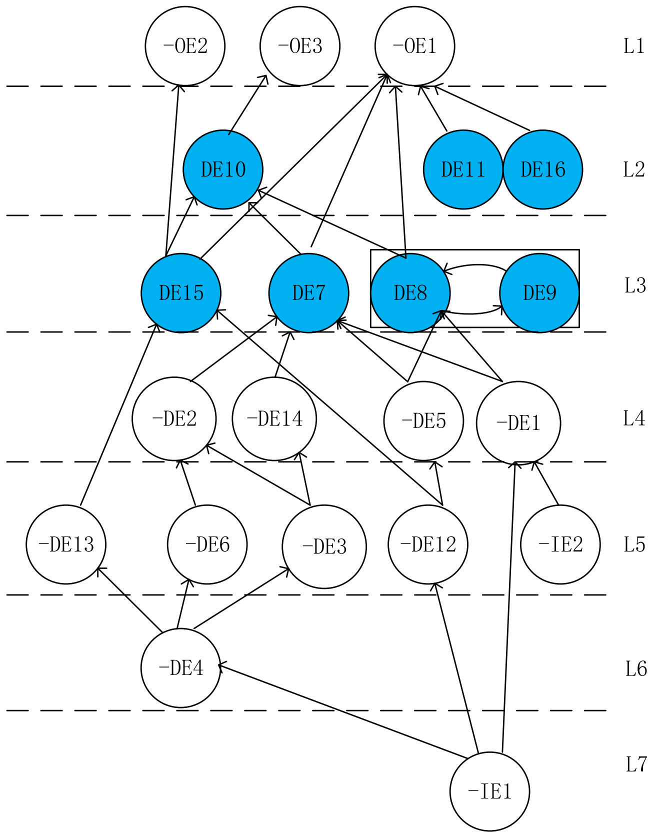


**Fig. 5.** Digraph for the limit value $|C_{ij}| = 3.41$– with 30%.

**Table 5**
Forecasted scenario-simulation for IE2 = 0 and IE2 = 1.

| | S0 | S1 |
|---|---|---|
| IE1 | 0.5000 | 0.5000 |
| IE2 | 0 | 1 |
| DE1 | 0.6351 | 0.9367 |
| DE2 | 0.4228 | 0.9037 |
| DE3 | 0.2575 | 0.8307 |
| DE4 | 0.5096 | 0.9657 |
| DE5 | 0.5837 | 0.9404 |
| DE6 | 0.1787 | 0.6670 |
| DE7 | 0.5000 | 0.5000 |
| DE8 | 0.5000 | 0.5000 |
| DE9 | 0.5000 | 0.5000 |
| DE10 | 0.7119 | 0.9900 |
| DE11 | 0.4992 | 0.9731 |
| DE12 | 0.4270 | 0.9217 |
| DE13 | 0.1405 | 0.6175 |
| DE14 | 0.5945 | 0.9672 |
| DE15 | 0.6831 | 0.7838 |
| DE16 | 0.7066 | 0.9918 |
| OE1 | 0.2092 | 0.9731 |
| OE2 | 0.3791 | 0.9555 |
| OE3 | 0.7732 | 0.9992 |

dynamic events related to system vulnerability are in a state of unfavorable influence on the outcome events (DE1 = DE5 = 0, DE7 = DE8 = DE9 = DE10 = DE15 = DE16 = 1), and the impact of human casualty (OE1), economic loss (OE2) and social panic (OE3) is minimized.

Outcome events can also be used to analyze the direct impact of supplementary initial and dynamic events on specific outcome events (Tables 7 and 8).

The initial probability of IE1, DE7, DE8, and DE9 obtained by the ROC method in Table 3 is 100%, so they are not included in the influence table. According to Table 7, the timely shutdown of metros is the event that has the most significant impact on human casualties. First-aid equipment in the metro and timely government guidance of public opinion had a slight effect on reducing overall deaths.

In Table 8, continuous rainfall and building damage after flooding disasters cause heavy economic loss. Similarly, the government's prompt guidance of public opinion and the provision of first-aid equipment in metro cars were the least damaging events to the economy.

According to Table 9, the government's prompt guidance of public opinion significantly alleviates social panic, which is much higher than in other events. Emergency equipment in metro cars has minimal impact on alleviating social panic.

According to Table 6 through Table 9, the metro company issued a timely notice of shutdown through the two analysis methods, which can significantly reduce casualties. The government promptly guided public opinion, which has the most significant influence on alleviating social panic. The traffic system disruption, communication, efficient rescue, assistance from humanitarian aid, and emergency medical treatment significantly impact economic losses.

## 4. Analysis and results

### 4.1. Comparison with other scenario-based methods

To further verify the reliability of the proposed method, we compared the cascading failure scenarios of the Bayesian network (BN) model and the ROC-based CIA-ISM. BN model, a scenario-based method, has been widely adopted for maritime accidents [44], blowout accidents [45], construction projects [46], and deep learning [47]. The ten cases [2–4,6] are collected by using the BN model. The events and prior probabilities are given in Tables 2 and 3. Next, the conditional probabilities between them can be obtained from Tables 10–12.

Figs. 6, 8, and 10 present the scenarios of three outcome events using the Bayesian Network model. Figs. 7, 9, and 11 present the scenarios of three outcome events using the ROC-based CIA-ISM.

A comparison of Figs. 6 and 7 reveals that the coupling relationship between events in Fig. 7 is more complicated. In both figures, extreme rainfall (IE1) affects the outcome events through cascading relationships. For example, in Fig. 6, extreme rainfall caused damage to the metro system and surrounding buildings (DE2), resulting in casualties (OE1). However, from the real case situation, the reason for the destruction of buildings is the widespread flooding (DE6) in the subway station area caused by the persistent rain (DE4). Likewise, extreme rainfall hinders the effectiveness of rescue teams, which in turn has an impact on casualties (OE1). Finally, the breakdown of the subway drainage system (DE13) exacerbated the casualties. But in this case, the metro company did not release timely notification of shutdown (DE15), which was the most significant cause of casualties. After the rainfall in Zhengzhou city reached a peak at 4 pm on July 20, 2021, many water inflows occurred on Metro Line 5. The subway was stopped 2 h after the rain flooded, and the best stop-loss opportunity was missed. The cross-impact relationship in Fig. 6 does not show a cascade path for subway outages. In Fig. 7, the failure of each subsystem of the subway system, such as the ventilation system (DE14), the drainage system (DE13) and the power system (DE12), will affect casualties, which is consistent with the actual situation. In this case, the ground transportation system (DE1) has a significant impact on casualties, and this cross-impact relationship is well demonstrated in Fig. 7. Likewise, persistent rain (DE4) had a positive effect on the paralysis of the drainage system (DE13), large-scale flooding (DE6), and component damage (DE3), which was consistent with the reality. The roles of social assistance (DE8) and Medicare (DE9) are not represented in Fig. 6.

From IE1 to OE2, the complexity of the coupling relationship in Figs. 8 and 9 is similar. In Fig. 8, extreme rainfall (IE1) can directly and indirectly affect economic losses (OE2). But in the selected case, extreme rainfall (IE1) affects the outcome events by affecting the dynamic events. In Fig. 8, building damage (DE2) and structural damage (DE3)

**Table 6**
Forecasted scenario-simulation for DE1 = DE5 = DE7 = DE8 = DE9 = DE10 = DE15 = DE16 = 1.

| | S0 | S1 | S2 | S3 | S4 | S5 | S6 | S7 | S8 | S9 |
|---|---|---|---|---|---|---|---|---|---|---|
| IE1 | 0.5000 | 0.5000 | 0.5000 | 0.5000 | 0.5000 | 0.5000 | 0.5000 | 0.5000 | 0.5000 | 0.5000 |
| IE2 | 0.5000 | 0.5000 | 0.5000 | 0.5000 | 0.5000 | 0.5000 | 0.5000 | 0.5000 | 0.5000 | 0.5000 |
| DE1 | 1 | 1 | 0 | 0 | 0 | 0 | 0 | 0 | 0 | 0 |
| DE2 | 0.8153 | 0.8454 | 0.8234 | 0.2738 | 0.2738 | 0.2738 | 0.7976 | 0.8412 | 0.8412 | 0.9987 |
| DE3 | 0.6955 | 0.7218 | 0.6874 | 0.1506 | 0.1506 | 0.1506 | 0.6698 | 0.7340 | 0.7340 | 0.9980 |
| DE4 | 0.9245 | 0.9334 | 0.9194 | 0.3375 | 0.3375 | 0.3375 | 0.9135 | 0.9393 | 0.9393 | 0.9999 |
| DE5 | 1 | 0 | 1 | 0 | 0 | 0 | 0 | 0 | 0 | 0 |
| DE6 | 0.4923 | 0.5071 | 0.4725 | 0.1027 | 0.1027 | 0.1027 | 0.4676 | 0.5318 | 0.5318 | 0.9886 |
| DE7 | 0 | 0 | 0 | 1 | 0 | 0 | 0 | 0 | 0 | 1 |
| DE8 | 0 | 0 | 0 | 0 | 1 | 0 | 0 | 0 | 0 | 1 |
| DE9 | 0 | 0 | 0 | 0 | 0 | 1 | 0 | 0 | 0 | 1 |
| DE10 | 0 | 0 | 0 | 0 | 0 | 0 | 1 | 0 | 0 | 1 |
| DE11 | 0.9566 | 0.9995 | 0.9446 | 0.5165 | 0.5165 | 0.5165 | 0.9504 | 0.1178 | 0.9866 | 0.9940 |
| DE12 | 0.8438 | 0.9286 | 0.8247 | 0.2746 | 0.2746 | 0.2746 | 0.8269 | 0.8680 | 0.8680 | 0.9993 |
| DE13 | 0.4383 | 0.8482 | 0.4222 | 0.0788 | 0.0788 | 0.0788 | 0.4133 | 0.4789 | 0.4789 | 0.9878 |
| DE14 | 0.9296 | 0.4575 | 0.9310 | 0.4231 | 0.4231 | 0.4231 | 0.9204 | 0.9424 | 0.9424 | 0.9998 |
| DE15 | 0 | 0 | 0 | 0 | 0 | 0 | 0 | 1 | 0 | 1 |
| DE16 | 0 | 0 | 0 | 0 | 0 | 0 | 0 | 0 | 1 | 1 |
| OE1 | 0.9817 | 0.9498 | 0.8917 | 0.2352 | 0.2352 | 0.2352 | 0.7470 | 0.1985 | 0.4403 | 0.0187 |
| OE2 | 0.8820 | 0.8440 | 0.8820 | 0.3020 | 0.3020 | 0.3020 | 0.7324 | 0.4089 | 0.5638 | 0.2952 |
| OE3 | 0.9975 | 0.9982 | 0.9975 | 0.7595 | 0.7595 | 0.7595 | 0.4049 | 0.9005 | 0.9587 | 0.3547 |

**Table 7**
OE1—Casualty (ordered influences table).

| Events | Name | $\|C_{ij}\|$ |
|---|---|---|
| DE15 | The metro company releases a timely notification of the shutdown. | 4.85 |
| IE2 | Metro flooding occurs during rush hours. | 3.63 |
| DE4 | Persistent rain. | 3.10 |
| DE13 | Surface and underground drainage systems are broken. | 2.97 |
| DE6 | Heavy rains cause widespread flooding in the area. | 2.86 |
| DE1 | The traffic system is paralyzed. | 2.76 |
| DE11 | The victims have a strong ability to help themselves. | 2.67 |
| DE14 | Metro ventilation system failure. | 2.59 |
| DE5 | Poor communication or interruption. | 2.51 |
| DE12 | The electricity supplies are disrupted. | 2.37 |
| DE3 | Failure of component or structure. | 2.31 |
| DE2 | Destruction of a building, such as a rupture, fall, and collapse. | 2.25 |
| DE16 | Metros are equipped with first aid equipment. | 2.19 |
| DE10 | The government guided public opinion and defused public discontent effectively. | 2.14 |

**Table 8**
OE2—Economic losses (ordered influence table).

| Events | Name | $\|C_{ij}\|$ |
|---|---|---|
| DE4 | The rain has been continuous. | 5.48 |
| DE2 | Destruction of a building, such as a rupture, fall, and collapse. | 4.12 |
| DE15 | The metro company issued a timely notice of the shutdown. | 3.44 |
| DE13 | Surface and underground drainage systems are broken. | 3.28 |
| DE6 | Heavy rains caused widespread flooding in the area. | 3.13 |
| DE1 | The transport system was paralyzed, hampering rescue efforts. | 3.00 |
| DE3 | Failure of component or structure. | 2.88 |
| DE14 | Metro ventilation system failure. | 2.77 |
| DE5 | Poor communication or interruption. | 2.67 |
| DE12 | The electricity supply was disrupted. | 2.48 |
| IE2 | Metro flooding occurs during rush hours. | 2.39 |
| DE11 | The trapped people have a strong ability to help themselves. | 2.31 |
| DE16 | Metro cars are equipped with first aid equipment. | 2.24 |
| DE10 | The government promptly guided public opinion. | 2.16 |

caused by extreme rainfall (IE1) increase economic losses (OE2). In the case of Zhengzhou metro flooding, timely shutdown of the subway (DE15) is the most direct way to reduce economic losses. The failure of various subsystems caused by persistent rain (DE4) is also an important reason for increased economic losses. The above case can be clearly presented in Fig. 9.

A comparison of Figs. 10 and 11 shows that the coupling relationship between events in Fig. 11 is more complicated. Building damage (DE2)

**Table 9**
OE3—Social panic (ordered influence table).

| Events | Name | $\|C_{ij}\|$ |
|---|---|---|
| DE10 | The government promptly guided public opinion. | 8.21 |
| DE4 | The rain has been continuous. | 3.67 |
| DE15 | The metro company issued a timely notice of the shutdown. | 3.06 |
| DE1 | The transport system was paralyzed, hampering rescue efforts. | 2.91 |
| DE6 | Heavy rains caused widespread flooding in the area. | 2.78 |
| DE13 | Surface and underground drainage systems are broken. | 2.67 |
| IE2 | Metro flooding occurs during rush hours. | 2.56 |
| DE11 | The trapped people have a strong ability to help themselves. | 2.46 |
| DE14 | Metro ventilation system failure. | 2.37 |
| DE5 | Poor communication or interruption. | 2.20 |
| DE12 | The electricity supply was disrupted. | 2.13 |
| DE3 | Failure of component or structure. | 2.06 |
| DE2 | Destruction of a building, such as a rupture, fall, and collapse. | 1.99 |
| DE16 | Metro cars are equipped with first aid equipment. | 1.92 |

caused by extreme rainfall (IE1), such as ventilation towers and retaining walls will affect social panic directly (OE3). But in this case, DE2 affects OE3 indirectly. After passengers are trapped, the rescue teams (DE7) and emergency medical care (DE9) can effectively alleviate social panic (OE3). In addition, the number of trapped persons (IE2) also had a positive effect on public panic. In actual situations, the government's function of guiding public opinion (DE10) is the most critical factor in alleviating public panic. Timely announcement of rescue progress (DE7), social assistance (DE8), medical security (DE10) and the degree of damage to the subway system (DE2, DE3, DE5, DE6, DE12, DE13, DE14) can effectively eliminate public panic. Fig. 10 shows, in a limited way, the impact of events such as building breakages on social panic. On the contrary, Fig. 11 clearly demonstrates the real situation of the cascading failure of social panic (OE3).

### 4.2. Implications

According to the metro flooding cases over the years, event sets are selected, most of which are related to the causes, system vulnerability, and emergency management of metro flooding [6,3,4]. An expert team was established by relevant personnel (such as emergency management professionals and first-line rescue workers) to evaluate the causal relationship between the two events, rank the importance of the events, and calculate the initial probability of the events using the ROC method. The estimation matrix and the initial probability were taken as the input of the cross-impact process, and a cross-impact matrix was established. The

**Table 10**
Conditional probability of OE1.

| Events | States[8] | Probability | Events | States | Probability | Events | States | Probability | Events | States | Probability |
|---|---|---|---|---|---|---|---|---|---|---|---|
| IE1 | 01 | 0%100% | DE4 | 01 | 37%63% | DE9 | 01 | 38%62% | DE14 | 01 | 99%1% |
| IE2 | 01 | 50%50% | DE5 | 01 | 99%1% | DE10 | 01 | 45%55% | DE15 | 01 | 68%32% |
| DE1 | 01 | 20%80% | DE6 | 01 | 8%92% | DE11 | 01 | 63%37% | DE16 | 01 | 8%92% |
| DE2 | 01 | 32%68% | DE7 | 01 | 5%95% | DE12 | 01 | 99%1% | OE1 | 01 | 34%66% |
| DE3 | 01 | 37%63% | DE8 | 01 | 99%1% | DE13 | 01 | 5%95% | | | |

[8] 0 represents none occur; 1 represents occur.

**Table 11**
Conditional probability of OE2.

| Events | States | Probability | Events | States | Probability | Events | States | Probability | Events | States | Probability |
|---|---|---|---|---|---|---|---|---|---|---|---|
| IE1 | 01 | 0%100% | DE4 | 01 | 38%62% | DE9 | 01 | 38%62% | DE14 | 01 | 99%1% |
| IE2 | 01 | 50%50% | DE5 | 01 | 99%1% | DE10 | 01 | 46%54% | DE15 | 01 | 69%31% |
| DE1 | 01 | 24%76% | DE6 | 01 | 8%92% | DE11 | 01 | 63%37% | DE16 | 01 | 8%92% |
| DE2 | 01 | 31%69% | DE7 | 01 | 5%95% | DE12 | 01 | 99%1% | OE2 | 01 | 8%92% |
| DE3 | 01 | 37%63% | DE8 | 01 | 99%1% | DE13 | 01 | 64%36% | | | |

**Table 12**
Conditional probability of OE3.

| Events | States | Probability | Events | States | Probability | Events | States | Probability | Events | States | Probability |
|---|---|---|---|---|---|---|---|---|---|---|---|
| IE1 | 01 | 0%100% | DE4 | 01 | 43%57% | DE9 | 01 | 45%55% | DE14 | 01 | 92%8% |
| IE2 | 01 | 50%50% | DE5 | 01 | 92%8% | DE10 | 01 | 47%53% | DE15 | 01 | 71%29% |
| DE1 | 01 | 31%69% | DE6 | 01 | 92%8% | DE11 | 01 | 59%41% | DE16 | 01 | 92%8% |
| DE2 | 01 | 41%59% | DE7 | 01 | 20%80% | DE12 | 01 | 92%8% | OE3 | 01 | 60%40% |
| DE3 | 01 | 44%56% | DE8 | 01 | 92%8% | DE13 | 01 | 20%80% | | | |

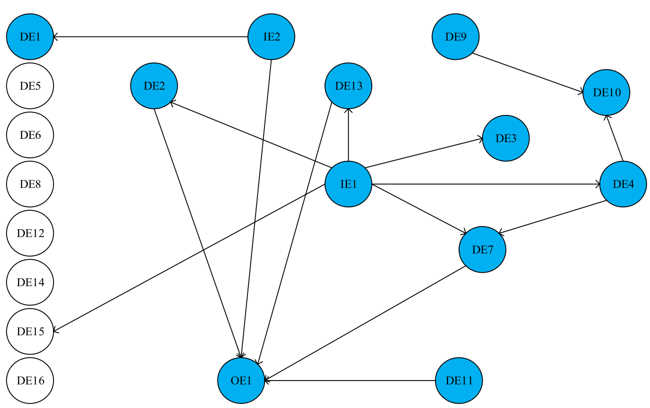


**Fig. 6.** BN network of OE1.

top 10 and 30% of the most significant impacts were extracted, and the causality of events was expressed structurally based on the interpretative structure model. The ROC-based CIA-ISM is adopted to effectively evaluate the nodes of system vulnerability of metro flooding through the scenario inference of the "7.20" metro flooding disaster in Zhengzhou. The model can directly represent the evolution scenarios of cascading failure and select the nodes of system vulnerability to assess their reliability.

In this article, timely notification of the shutdown has the most complex coupling relationships in the cascading failure process in metro systems. The efficiency of several critical emergency measures was assessed, and it was found that the events with the greatest influence on the three outcome events (OE1, OE2, OE3) are DE15, DE4, and DE10, based on the ranking of cross-impact value. For emergency events, DE15 and DE10 have a significant effect on the outcome events. Through simulation, the probability of casualties, property losses, and social panic decrease by 96.3%, 58.58%, and 64.28%, respectively, where main emergency measures are in effect. Furthermore, the ROC-based CIA-ISM model is compared with the other scenario-based approach to

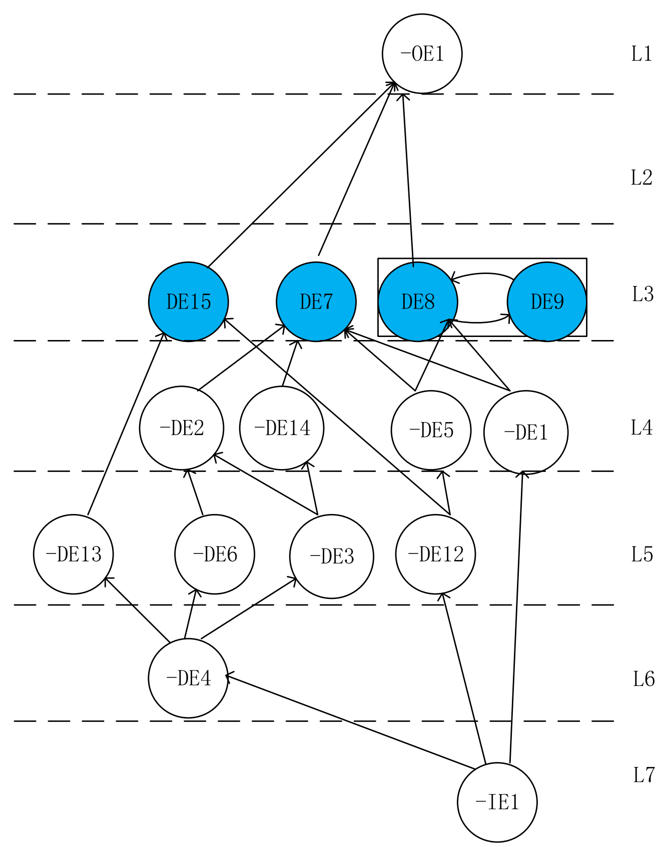


**Fig. 7.** ROC-based CIA-ISM of OE1.

verify its superiority in cascading failure analysis.

Through the above analysis, some countermeasures and suggestions can be put forward. Metro flooding disaster emergency preparation is of

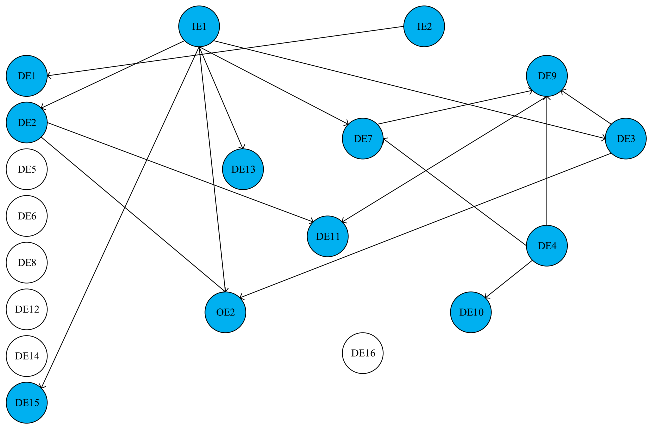


**Fig. 8.** BN network of OE2.

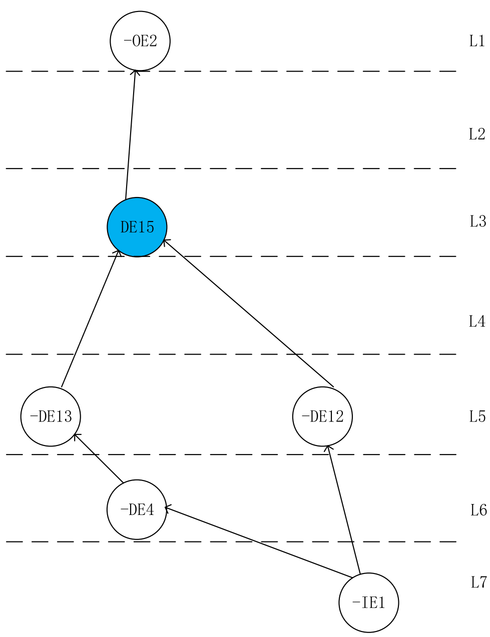


**Fig. 9.** ROC-based CIA-ISM of OE2.

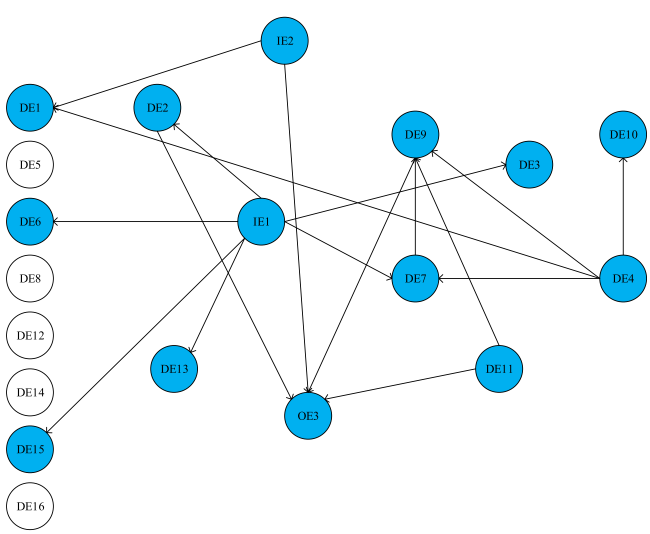


**Fig. 10.** BN network of OE3.

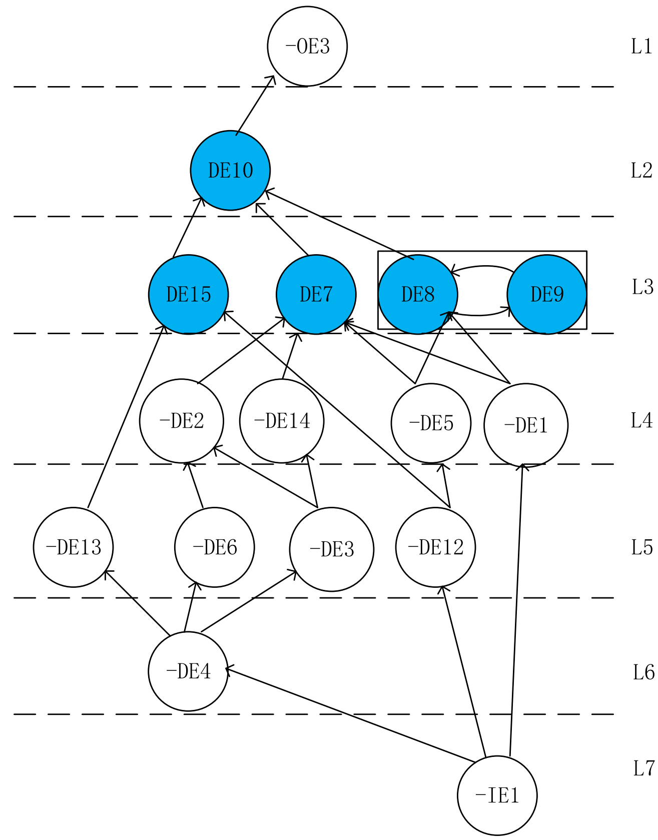


**Fig. 11.** ROC-based CIA-ISM of OE3.

great significance to guide on-site disposal before and after disaster, and all sectors of society should properly deal with metro flooding disasters to reduce losses. After heavy rain, when the precipitation reaches the warning line, the metro company should issue a timely notification of shutdown so as to reduce casualties to the greatest extent. Ensuring smooth traffic system flow and efficient rescue by a professional rescue team is also a key factor in reducing casualties. The government should give priority to the guidance of public opinion. Therefore, it is necessary to disclose the disaster information timely. We propose to improve the emergency capacity to withstand metro flooding through explicit legislation in the new urban plan. In Scenario 9 of Table 6, casualty, property loss, and social panic are minimized where all emergency management measures are in effect, indicating that the measures must be supplemented with each other. Regularly checking the underground drainage network before the rain season could help to ensure its proper operation during torrential floods [6]. We suggest developing a metro flood monitoring and warning system and promptly delivering risk information to citizens through communication companies [6].

Moreover, hard adaptation strategies play an important role in flood control [48]. Compared to emergency measures, hard adaptation exhibits the advantages of high benefit and low cost in loss reduction [49,50]. Accordingly, we propose to raise exits to stop surface water intrusion into metro stations [51]. It is necessary to install water-stop plates at the low-lying stations [50,51]. In addition, the height of ventilation towers should be raised, and stop-flood boards are required if the vents are connected to the ground. These structural measures are recommended to prevent urban flooding from rushing into metro stations.

### 4.3. Limitations

There are some drawbacks in this study. For one thing, the ROC-based CIA-ISM approach effectively deconstructs the cascading failure process in metro systems under extreme rainfall conditions. However, the numerical ordering of the event's shortcomings is due to the subjective assessment. Random Forests (RF) is a powerful statistical classification used to rank the events based on their Gini index [52]. Thus, future research will modify the events ranking process based on the RF.

For another, the structural events, such as the exit height of metro stations and the height of ventilation towers, are not involved in the risk indicator system due to data acquisition limitations. However, these events also affected metro systems' cascading failure under extreme rainfall conditions [6]. Therefore, future research will employ text mining to build the event set.

## 5. Conclusions

Based on the analysis of the "7.20" metro flooding in Zhengzhou city, the events related to metro flooding are selected to form an event set. Most events relate to metro flooding, heavy rain secondary disaster, and system vulnerability. The initial probability of the event set can be obtained by the experts' rank of ROC and probability elicitation. Experts in emergency management were invited to form a panel with first responders to provide consistent estimates of the causal relationship between the two events. The estimated results are input to the cross-impact process in matrix form. A cross-impact matrix was established based on the CIA, and some of the most significant influence was extracted (top 10 and 30% were extracted in this paper). The extracted influence values are expressed structurally through the ISM. The scenario deduction of the "7.20" metro flooding disaster in Zhengzhou shows that the ROC-based CIA-ISM can effectively deconstruct the cascading failure mode of metro flooding and evaluate the vulnerability of system nodes. After the above analysis and research, this paper draws the following conclusions.

(1) The initial probability of events is obtained in a probabilistic elicitation way by ranking the ROC method so that experts are only subjected to minimal cognitive bias and have strong robustness. In addition, the ROC method can reduce the subjective influence on the initial probability assignment of events, effectively mitigate the impact of external events on the event set, and enhance the comprehensiveness of events.
(2) Based on the scenario inference process, the ROC-based CIA-ISM can directly reflect the coupling relationship between events, the propagation path, and the relationship between different levels, realizing the highly structured expression of the disaster evolution process to block the disaster transmission chain quickly and effectively. By evaluating the vulnerability nodes related to metro flooding accidents, the reliability of various emergency management measures can be identified to reduce accident losses and help decision-makers propose more accurate risk control strategies.
(3) Taking the "7.20" metro flooding disaster in Zhengzhou as a case study, the cascading failure model of metro flooding disasters can effectively evolve the disaster process and identify the coupling relationship between key vulnerability nodes. The model's effectiveness is verified by scenario deduction and case simulation, and the prediction scenario is consistent with the actual situation. According to the natural disaster situation and scenario simulation results, it is helpful to put forward specific measures and provide reference for system vulnerability assessment and emergency management.

For future research, the application of causal inference is needed for cascading failure analysis in complex systems. Instead of just scenario inference, the cascading process will be deconstructed by applying the three levels of causal inference, which are association, intervention, and counterfactuals. Moreover, the decoupling research of cascading failure mode in complex systems will be done in the future studies. Finally, it is worth noting that the causal inference enables a better evaluation of cascading mode and decoupling process.

## CRediT authorship contribution statement

**Zhen Yang:** Conceptualization, Methodology. **Xiaobin Dong:** Investigation, Data curation, Writing – original draft. **Li Guo:** Supervision, Writing – review & editing.

## Declaration of Competing Interest

We have no conflict of interest with anyone.

## Data Availability

The authors do not have permission to share data.

## References


[1] Lyu HM, Wang GF, Cheng WC, Shen SL. Tornado hazards on June 23 in Jiangsu Province, China: preliminary investigation and analysis. Nat Hazards 2017;85(1): 597–604.
[2] Shen SL, Wu HN, Cui YJ, Yin ZY. Long-term settlement behaviour of metro tunnels in the soft deposits of Shanghai. Tunneling Undergr Space Technol 2014;40: 309–23.
[3] Lyu HM, Sun WJ, Shen SL, Arulrajah A. Flood risk assessment in metro systems of mega-cities using a GIS-based modeling approach. Sci Total Environ 2018;626: 1012–25.
[4] Lyu HM, Shen SL, Zhou AN, Zhou WH. Flood risk assessment of metro systems in a subsiding environment using the interval FAHP-FCA approach. Sustain Cities Soc 2019;50:101682.
[5] Huddleston P, Smith T, White I, Elrick-Barr C. Adapting critical infrastructure to climate change: a scoping review. Environ Sci Policy 2022;135:67–76.
[6] Wang G, Liu L, Shi P, Zhang G, Liu J. Flood risk assessment of metro system using improved trapezoidal fuzzy AHP: a case study of Guangzhou. Remote Sens 2021;13 (24):5154.
[7] Mahmoud MS, Xia Y, Mahmoud MS, Xia Y. Chapter 9—cyberphysical security methods. Networked control systems. Butterworth-Heinemann; 2019. p. 389–456.
[8] Jansen R, Yu H, Greenbaum D, Kluger Y, Krogan NJ, Chung S, Gerstein M. A Bayesian networks approach for predicting protein-protein interactions from genomic data. Science 2003;302(5644):449–53.
[9] Sachs K, Perez O, Pe'er D, Lauffenburger DA, Nolan GP. Causal protein-signaling networks derived from multiparameter single-cell data. Science 2005;308(5721): 523–9.
[10] Li R, Pei S, Chen B, Song Y, Zhang T, Yang W, Shaman J. Substantial undocumented infection facilitates the rapid dissemination of novel coronavirus (SARS-CoV-2). Science 2020;368(6490):489–93.
[11] Pearl J. Causality. Cambridge university press; 2009.
[12] Textor J, Van der Zander B, Gilthorpe MS, Liśkiewicz M, Ellison GT. Robust causal inference using directed acyclic graphs: the R package 'ditty. Int J Epidemiol 2016; 45(6):1887–94.
[13] Li A, Pearl J. Unit selection with causal diagram. Proc AAAI Conf Artif Intell 2022; 36(5):5765–72.
[14] Petri CA. Communication with Automata. DTIC Research Report. DTIC; 1966, AD0630125.http://refhub.elsevier.com/S2212-0416(20)30162-5/h0315.
[15] Desel J, Juhás G. What is a Petri net?" informal answers for the informed reader. Unifying petri nets. Berlin, Heidelberg: Springer; 2001. p. 1–25.
[16] David R, Alla H. Discrete, continuous, and hybrid petri nets, 1. Berlin: Springer; 2010. p. 17–130.
[17] Dynkin EB. Markov processes. Markov processes. Berlin, Heidelberg: Springer; 1965. p. 77–104.
[18] Norris JR, Norris JR. Markov chains, 2. Cambridge university press; 1998.
[19] Rabiner L, Juang B. An introduction to hidden Markov models. IEEE ASSP Mag 1986;3(1):4–16.
[20] Fan L, Su H, Wang W, Zio E, Zhang L, Yang Z, Zhang J. A systematic method for the optimization of gas supply reliability in natural gas pipeline network based on Bayesian networks and deep reinforcement learning. Reliab Eng Syst Saf 2022;225: 108613.
[21] Zhang Q, Xu N, Ersoy D, Liu Y. Manifold-based conditional Bayesian network for aging pipe yield strength estimation with non-destructive measurements. Reliab Eng Syst Saf 2022;223:108447.
[22] Liu S, Li W, Gao P, Sun Y. Modeling and performance analysis of gas leakage emergency disposal process in gas transmission station based on stochastic petri nets. Reliab Eng Syst Saf 2022:108708.
[23] Liu J, Zhai C, Yu P. A probabilistic framework to evaluate seismic resilience of hospital buildings using Bayesian networks. Reliab Eng Syst Saf 2022:108644.
[24] Silva FA, Brito C, Araújo G, Fé I, Tyan M, Lee JW, Maciel PRM. Model-driven impact quantification of energy resource redundancy and server rejuvenation on the dependability of medical sensor networks in smart hospitals. Sensors 2022;22 (4):1595.

[25] Ye J, Xu Z, Gou X. An adaptive grey-markov model based on parameters Self-optimization with application to passenger flow volume prediction. Expert Syst Appl 2022;202:117302.
[26] Li S, Wu T. Deep reinforcement learning-based decision support system for transportation infrastructure management under hurricane events. Struct Saf 2022;99:102254.
[27] Ghoushchi SJ, Bonab SR, Ghiaci AM, Haseli G, Tomaskova H, Hajiaghaei-Keshteli M. Landfill site selection for medical waste using an integrated SWARA-WASPAS framework based on spherical fuzzy set. Sustainability 2021;13(24):13950.
[28] Wang R, Wang E, Li L, Li W. Evaluating the effectiveness of the COVID-19 emergency outbreak prevention and control based on CIA-ISM. Int J Environ Res Public Health 2022;19(12):7146.
[29] Chen T, Sun H, Tai KF, Heng CK. Analysis of the barriers to implementing building integrated photovoltaics in Singapore using an interpretive structural modelling approach. J Clean Prod 2022;365:132652.
[30] Fu X, Wang H, Shi P, Zhang X. Teegraph: a blockchain consensus algorithm based on TEE and DAG for data sharing in IoT. J Syst Archit 2022;122:102344.
[31] Li XY, Liu Y, Lin YH, Xiao LH, Zio E, Kang R. A generalized petri net-based modeling framework for service reliability evaluation and management of cloud data centers. Reliab Eng Syst Saf 2021;207:107381.
[32] Rahnamay-Naeini M, Hayat MM. Cascading failures in interdependent infrastructures: an interdependent Markov-chain approach. IEEE Trans Smart Grid 2016;7(4):1997–2006.
[33] Kaviyani-Charati M, Ghodsypour SH, Hajiaghaei-Keshteli M. Impact of adopting quick response and agility on supply chain competition with strategic customer behavior. Sci Iran 2022;29(1):387–411.
[34] Edwards W, Barron FH. SMARTS and SMARTER: improved simple methods for multiattribute utility measurement. Organ Behav Hum Decis Process 1994;60(3):306–25.
[35] Barron FH, Barrett BE. Decision quality using ranked attribute weights. Manag Sci 1996;42(11):1515–23.
[36] Roberts R, Goodwin P. Weight approximations in multi-attribute decision models. J Multi Criteria Decis Anal 2002;11(6):291–303.
[37] Urlainis A, Ornai D, Levy R, Vilnay O, Shohet IM. Loss and damage assessment in critical infrastructures due to extreme events. Saf Sci 2022;147:105587.
[38] Jaspersen JG, Montibeller G. Probability elicitation under severe time pressure: a rank-based method. Risk Anal 2015;35(7):1317–35.
[39] David HA, Nagaraja HN. Order statistics. John Wiley & Sons; 2004.
[40] Ludke RL, Stauss FF, Gustafson DH. Comparison of five methods for estimating subjective probability distributions. Organ Behav Hum Perform 1977;19(1):162–79.
[41] Bañuls VA, Turoff M, Hiltz SR. Collaborative scenario modeling in emergency management through cross-impact. Technol Forecast Soc Change 2013;80(9):1756–74.
[42] Stergiopoulos G, Kotzanikolaou P, Theocharidou M, Gritzalis D. Risk mitigation strategies for critical infrastructures based on graph centrality analysis. Int J Crit Infrastruct Prot 2015;10:34–44.
[43] Zhang Y, Weng WG, Huang ZL. A scenario-based model for earthquake emergency management effectiveness evaluation. Technol Forecast Soc Change 2018;128:197–207.
[44] Fu S, Yu Y, Chen J, Xi Y, Zhang M. A framework for quantitative analysis of the causation of grounding accidents in arctic shipping. Reliab Eng Syst Saf 2022:108706.
[45] Meng X, Chen G, Zhu J, Li T. Application of integrated STAMP-BN in safety analysis of subsea blowout preventer. Ocean Eng 2022;258:111740.
[46] Arabi S, Eshtehardian E, Shafiei I. Using Bayesian networks for selecting risk-response strategies in construction projects. J Constr Eng Manag 2022;148(8):04022067.
[47] Zhou T, Han T, Droguett EL. Towards trustworthy machine fault diagnosis: a probabilistic Bayesian deep learning framework. Reliab Eng Syst Saf 2022;224:108525.
[48] Du S, Scussolini P, Ward PJ, Zhang M, Wen J, Wang L, Aerts JC. Hard or soft flood adaptation? Advantages of a hybrid strategy for Shanghai. Glob Environ Chang 2020;61:102037.
[49] Yin J, Ye M, Yin Z, Xu S. A review of advances in urban flood risk analysis over China. Stoch Environ Res Risk Assess 2015;29(3):1063–70.
[50] Wang G, Liu Y, Hu Z, Zhang G, Liu J, Lyu Y, Liu L. Flood risk assessment of subway systems in metropolitan areas under land subsidence scenario: a case study of Beijing. Remote Sens 2021;13(4):637.
[51] Aoki Y, Yoshizawa A, Taminato T. Anti-inundation measures for underground stations of Tokyo Metro. Procedia Eng 2016;165:2–10.
[52] Cutler DR, Edwards Jr TC, Beard KH, Cutler A, Hess KT, Gibson J, Lawler JJ. Random forests for classification in ecology. Ecology 2007;88(11):2783–92.

Zhen Yang is a professor at Xi 'an University of Architecture and Technology. His research interestsinclude safety big data and risk management, and AI-assisted safety system engineering. E-mail:yangzhen@xauat.edu.cn